VII International Congress on Architectural Envelopes
Title of the paper

AMANAC-session: Sol-gel based coatings for low ice-spreading on HVAC systems

Jacob A. Hansen[1], Stefan Holberg[1], Ricardo Losada[1], N. Arconada[2], M. Hernaiz[2], E. Rodriguez[2], R. Ortiz[2]

[1]Danish Technoloigcal Institute, Kongsvang Alle 29, 8000 Aarhus C, Denmark
[2] IK4- Tekniker, Iñaki Goenaga 5, 20600 Éibar, Basque Country, Spain
e-mail: jbha@dti.dk

Key words: Anti-ice, Sol-gel coatings, Laser ablation technology, Surface micro-structuring, HVAC.

Abstract

Frost formation and growth on heat exchanger surfaces in refrigeration, ventilation and air conditioning systems has posed a challenge to heat transfer engineers for decades. Frost buildup causes an increase in the airside pressure drop and thermal resistance, yielding a substantial decrease in operational efficiency. Freezing starts in surface defects owing to their geometric singularity and low free energy barrier for heterogeneous ice nucleation. This triggers the formation of a freezing weave, which eventually spreads over the entire surface. The development of a realistic laboratory test has proven to be crucial for the better understanding of the freezing process. Herein, we investigated various hydrophobic coatings and related their surface properties with the frost spreading behavior. While complete freeze-depression is expected to maintain unrealistic, we demonstrate that hydrophobic coatings with defined surface properties significantly reduce frost spreading. This phenomenon, which has most likely been interpreted as freeze-depression in many occasions, we believe it could be exploitable industrially to extend defrosting intervals.

1 Introduction

Frost affects various devices such as airfoils, electrical power lines or pipelines. The present work originated from two specific heating and ventilation problems. The first is air-to-refrigerant heat exchangers of heat pumps using outside air as heat source (evaporator in Figure 1). The heat exchanger fins are cooled below 0°C when the outside temperature is below about 7°C. The second is air-to-air heat exchangers of heat recovery ventilation (HRV in Figure 1). At outside temperatures below about -3°C, the more humid outgoing air is cooled to temperatures below 0°C. In both cases, ice accumulates on the respective surfaces, impairing the heat transfer and requiring periodic defrosting by heating,

thus consuming energy. Periodic defrosting is also applied in other applications such as, for example, to deice wind turbine wings.

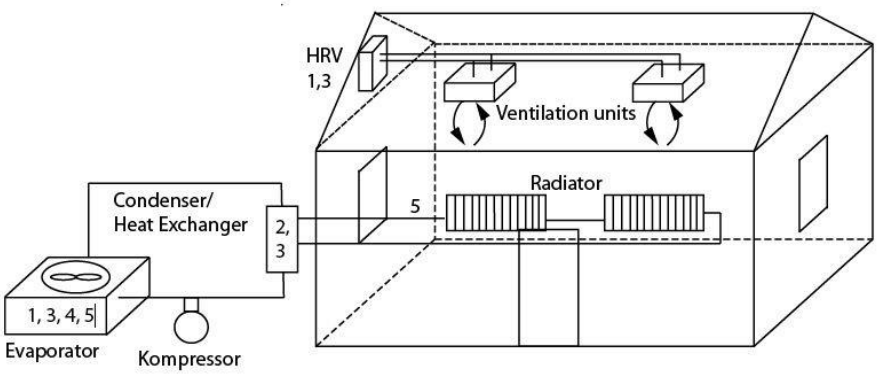

Figure 1: Schematic of a building with heat pump and heat recovery ventilation.

Scientists have put effort into anti-icing surfaces to reduce ice adhesion or retard the first ice nucleation on a wet surface [1] [2]. The efficiency of the frequently applied hydrophobic surfaces under conditions of high humidity, air flow or icing/deicing cycles has, however, been critically questioned [1-3]. Especially on superhydrophobic surfaces, water can possibly condense inside a microstructure in a Wenzel-regime, void superhydrophobicity and increase ice adhesion due to a larger contact area. The present study addresses the interplay between the surface properties and the interdroplet freezing phenomenon on hydrophobic surfaces. Our results demonstrate that hydrophobic surfaces with low contact angle hysteresis significantly reduce the frost spreading, which can be applied to extend the time period between defrosting cycles and allows to consider new strategies when developing anti-ice surfaces.

2 Coatings for slow frost spreading

Hydrophobic and superhydrophobic coatings change the wetting of a surface by water. The wettability of a solid surface is a combined result of the surface free energy and special topographic features. By modifying the surface free energy of surfaces with similar morphology or by changing the morphology of surfaces with the same free energy is possible to fabricate surfaces with different wettability. In the ideal situation, the water droplets run off the surface before having a chance to freeze.

2.1 Investigated coatings

To analyze the frost spreading rate on HVAC surfaces, both non-structured (smooth) and structured surfaces have been studied. The following non-structured surfaces were investigated: Hydrophobic polymer films: Polypropylene (PP), and fluorinated ethylene propylene (FEP), and cross-linked polydimethylsiloxane (silicone rubber, bulk-PDMS). Hydrophobic Coatings: We prepared the smooth organic-inorganic hybrid coatings labelled herein Coating 1, 2, 3 and 4 from organosilanes with optionally additional organic monomers. The hydrophobic surface of Coating 1 and Coating 3 is provided by a polydimethylsiloxane additive. Coating 2 is prepared identical to coating 1, but without the PDMS additive. Coatings 1, 2 and 3 are similar to already published coatings [4].

Coating 4 was prepared using TEOS as the inorganic precursor for the sol-gel synthesis and PFOTS as co-precursor to improve the water repellence of the surface. The synthesis was prepared in an acidic media by addition of a mixture of water/nitric acid. Coating 4 was deposited by dip-coating onto aluminium substrates at 300 mm/s at controlled temperature and humidity and treated at 150 ºC for 1 hour. Coatings 1, 2 and 3 were applied by spraying and cured at 200°C (Coating 1 and 2) and 140°C (Coating 3). Table 1 provides water contact angle measurements of the respective surfaces.

The structured superhydrophobic surfaces Coating 5 and Coating 6 were prepared by combining the sol-gel route similar to Coating 4 with a micro-structuring process in order to increase the hydrophobicity of the surfaces. The micro-structuring was performed by laser ablation directly onto the aluminum substrate. This texturization technique can be applied to fabricate three-dimensional micro- and nano-structures to change the wettability of surfaces by modification of its topography.

Laser texture parameters were optimized as a function to obtain minimum distance peak to peak and maximum distance peak to valley. Thus, pyramidal structures, coating 5, were prepared with reduced peak-peak distance to 15 and 20 µm and increased peak-valley height of 20 µm and lines structures, coating 6, with reduced peak-peak distance 50, 60, 70 µm and increased peak-valley height of 40 µm.

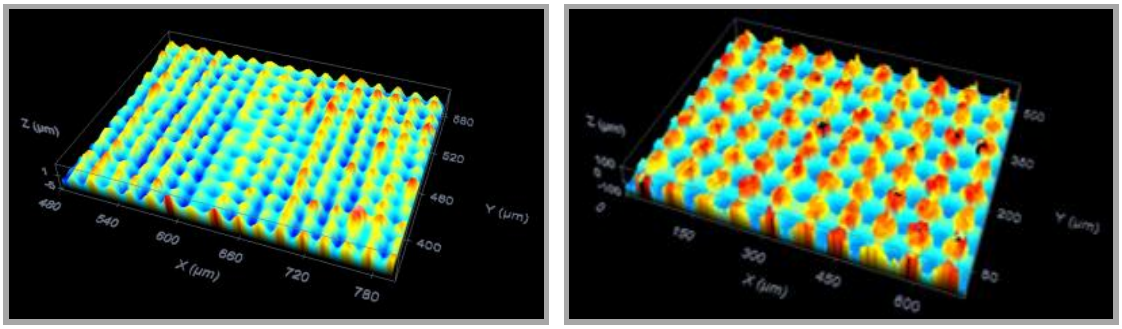

Figure 2: Pyramidal structure obtained by picoseconds laser and grid lines obtained by nanoseconds laser.

Finally, the structured substrates were coated with Coating 4. Table 1 provides water contact angle measurements of the respective structured surfaces.

2.2 Freezing tests

The frost spreading was investigated in a special ice test chamber. The test chamber (Figure 3, sample plate is mounted into the left wall) controls the environment. The temperature is hold at +12 °C, relative humidity at about 90%. There is a weak, undefined air flow downwards due to natural convection along the cold sample plate. In those experiments, where an air flow is specifically mentioned, a wing with an additional fan is mounted inside the box, parallel to the sample surface to enforces an upward air flow of about 1 m/s, reducing the humidity to about 60%.

The temperature of the sample plate surfaces is controlled by a cooling block (Cu-block with peltier element and thermo couple, see Figure 3, and Figure 4 eclipsed by the sample plate). The cooling block is connected to the sample plate through a thin ice film. Provided surface temperatures are cooling block temperatures. At the start of each experiment, the cooling block is placed outside the test box and is covered with water. The sample plates (101 x 152 mm) are with their backside placed on the cooling block and attached by freezing. The edge of the cooling block is throughout the whole experiments heated by a heating wire to temperatures above 0°C to prevent contact-freezing form the backside. By thawing tests performed at the end of each experiment, where we kept the ice covered

plate at -0.5°C for 15 min, we could confirm, that only a stripe of about 1 cm from edges was warmer than 0°C, the rest of the sample surface was below 0°C, see Figure 7. Thus, we expect a maximum error of 0.5°C for the whole sample surface except the area close to the edges. A camera inside the test box continuously monitors the sample plate surface.

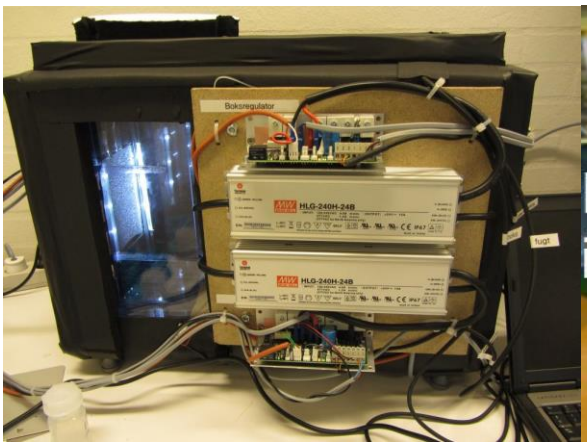

Figure 3: Ice test chamber.

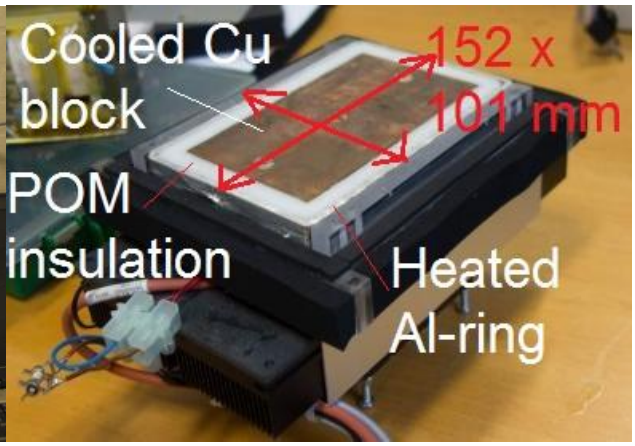

Figure 4: Cooling block for the ice test chamber.

The cooling block with the sample plate is mounted into an opening in the wall of the box, with the sample plate in vertical position. For all experiments, the sample plates are hold at -2°C until enough water has condensed on the plate to start running down in drops. Thereafter, the actual experiments starts. All experiments are carried out while water continuously condenses and drops run down.

3 Results

After the first occurrence of freezing, the further fate of the sample surfaces differs significantly. While bare metal plates almost instantly freeze completely, the frozen area growth slowly on hydrophobic surfaces. When carrying out above described experiments to determine the freezing temperature, the sample plates were hold at their respective freezing temperature for 20 min to roughly estimate the rate of frost growth. Selected samples were in a more precise experiment held at -4°C and freezing was induced by placing ice in the middle of the sample to start frost growth. In the first 20 min, the growth rate is more or less constant when calculating a linear growth rate of the radius of the frozen area. The results are summarized in table 1.

According to literature, frost spreads from a frozen drop to a neighboring liquid drop [5-6]. Water condenses faster on the frozen drop due to the lower vapour pressure of ice than for the liquid water at the same temperature. The frozen drop growth along the surface and finally touches a liquid drop. Due to the different vapour pressure, neighbouring liquid drops may even evaporate and contract.

A connection with the critical diameter d_{crit} for a water droplet to be big enough to start sliding down a vertical surface was proposed. The smaller d_{crit}, the slower the ice spreading, though no equation for the exact relation between dcrit and an ice-spreading rate was established. d_{crit} can be calculated from advancing and receding contact angles, see Figure 5. Simplified, the optimal surface should provide a low contact angle hysteresis (CAH). For a given CAH, the absolute contact angle values should be high.

$$Critical\ diameter = \sqrt{\left(\frac{24\ sin^3\theta adv\ \gamma(cos\theta rec - cos\theta adv)}{\pi\rho(1-cos\theta adv)^2(2+cos\theta adv)gsin\alpha}\right)}$$

Figure 5: Critical diameter d_{crit} at which a drop starts to slide down according to [6]. α: surface tilt angle (90° in our experiments), ρ: density of the liquid, γ: surface tension of the liquid, θadv and θrec are the respective contact angles, g: gravity acceleration.

Our results shown in Table 1 support the proposed trend. The contact angle data alone seems, however, not to be sufficient. Frost spreading on aluminum was significantly faster than on PP, despite similar d_{crit}.

Table 1: Frost spreading rate.

Surface	Water contact angle		Calc. crit. drop	Frost spreading rate	
	adv.	rec.	diam. dcrit	Rough estimation	Precise (-4 °C)
Bare carbon steel	69°	26°	5.1 mm	instantly, > 1 mm/s	
Bare aluminium	96°	50°	4.2 mm	instantly, > 1 mm/s	~3 mm/s
PP	96°	69°	3.9 mm	1 mm/s to 10 µm/s	
Coating 2	89°	73°	2.8 mm	1 mm/s to 10 µm/s	21 µm/s
Bulk PDMS	113°	88°	2.5 mm	slow, <10 µm/s	
FEP	114°	95°	2.1 mm	slow, <10 µm/s	
Coating 1	106°	96°	1.8 mm	slow, <10 µm/s	~4 µm/s
Coating 3	104°	95°	1.8 mm	slow, <10 µm/s	~2 µm/s
Coating 4	105°	95°	1.8 mm	slow, <10 µm/s	~3 µm/s
Coating 5	127°	90°	-	-	-
Coating 6	150°	138°	-	-	-

The frost spreading on the structured surfaces (superhydrophobic) has not yet been analyzed. According to literature [1], the main challenge is, in conditions of high humidity, to avoid that water condense inside the topographic features and the superhydrophobic properties collapse. We investigated the condensation behavior of the superhydrophobic coatings "Coating 5" and "Coating 6". The coatings maintain drop wise condensation and hydrophobic properties, see Figure 6. Even though receding and advancing contact angles are under condensation conditions are lower than the values provided by table 1 measured on a dry surface, our results indicates that even under condensation conditions, the water on these samples is, at least partly, in a Cassie-Baxter state (air-pocket state). Thus, the developed superhydrophobic surfaces have already overcome a main barrier for their application as anti-ice coatings. Nevertheless, further studies are required to analyze the frost spreading.

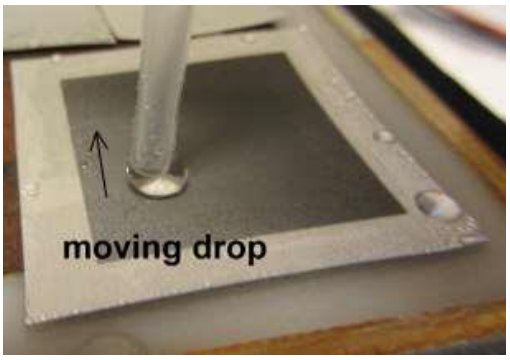

Figure 6: Micro-structured sample (Coating 6) tested under condensation conditions

In addition to the mechanism described in literature, the frost growth on smooth surfaces is in our experiments further affected by drops sliding down the surface. Drops that touch the frozen area freeze at the spot and enlarge it. Drops passing close to the frozen area temporarily clean that area from condensed water and delay frost growth (see Figure 7).

Frost spreading tests were also carried out with forced convection at a flow rate of 1 m/s, as is typical for heat exchangers. The tests were repeated four times with different plates. After a short induction period, ice spreads in each test run fast in direction along the flow (see Figure 9). In the other directions, spreading on hydrophobic surfaces is still slow. Thereby, growth is fastest in direction of the lowest humidity.
Thus, this phenomenon cannot be explained by the model outlined above. Frost starts even to grow several cm away from the point of initiation, while in between liquid water remains. Even though no flying ice crystals were visible, a plausible explanation is, that lose frost forms on top of the frozen droplets and is detached and transported by the flow.

Figure 7: Bare aluminium plate with a frost layer hold at -0.5°C for 15 min to verify contact with the cooling block. The edge is heated and thus ice free.

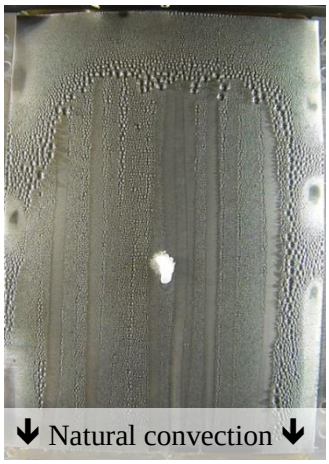

Figure 8: Aluminium plate with coating 3, 10 x 15 cm, hold at -4°C for 20 min after placing ice in the middle. Environment +12°C, ~90% relative humidity, continuous condensation.

Figure 9: Identical experiment as shown in Figure 8, but with forced upward airflow of 1 m/s and thus reduced relative humidity of ~60%.

4 Conclusions

Hydrophobic surfaces reduced the frost spreading rate by more than a factor of 1000 compared to bare aluminium. This effect can be exploited for heat exchangers at temperatures, where ice nucleation occurs at a low rate solely at isolated spots. The goal is to fabricate coatings which are durable in contact with water, have low contact angle hysteresis and high static contact angles. A drawback is the frost growth in direction of the airflow. Practical test have yet to reveal the precise effect on the defrosting intervals in realistic installations.
Moreover, the structured suprhydrophobic surfaces fabricated in the frame of this work, have shown promising results under condensation conditions tests under condensation. However, more detailed studies are required to analyze the frost growth on these structures.

Acknowledgements

The project "*Energy efficient heat exchangers for HVAC applications*" or EnE-HVAC is granted under the **Seventh Framework Programme, Theme EeB.NMP.2012-4**: Nanotechnology based approaches to increase the performance of HVAC systems.

Reference

[1] A.J. Meuler, G.H. McKinley, R.E. Cohen; *ACS Nano* 2010, 4 (12), 7048-7052.

[2] V. Stenzel, N. Rehfeld; *Functional Coatings*, Vincentz Network, Hannover, 2011, p. 91 - 106.

[3] S. Jung, M.K. Tiwari, N.V. Doan, D. Poulikakos, *Nat. Commun*. 2012, 3, article no. 615.

[4] C. Bischoff, S. Holberg. Repellent coating composition and coating, process for making and uses thereof. *Patent WO 2012/083970 A1* (2012).

[5] a) J.B. Boreyko, C.P. Collier. Delayed frost growth on jumping-drop superhydrophobic surfaces; *ACS Nano* 7 (2013), 1618.

b) X.M. Chen, R. Ma, H. Zhou, X. Zhou, L. Che, S. Yao, Z. Wang. Activating the microscale edge effect in a hierarchical surface for frosting suppression and defrosting promotion. *Sci. Rep*. 3 (2013), 2515.

[6] P. Kim, T-S. Wong, J. Alvarenga, M.J. Kreder, W.E. Adorno-Martinez, J. Aizenberg. Liquid-infused nanostructured surfaces with extreme anti-ice and anti-frost performance. *ACS Nano* 6(8) (2012), 6569